

Structural, Spectroscopic, Electrochemical and Computational Studies of C,C'-diaryl-*ortho*-carboranes, 1-(4-XC₆H₄)-2-Ph-1,2-C₂B₁₀H₁₀ (X = H, F, OMe, NMe₂, NH₂, OH and O⁻).

Mark A. Fox,^{a,*} Carlo Nervi,^{b,*} Antonella Crivello,^b Andrei S. Batsanov,^a Judith A. K. Howard,^a Kenneth Wade^a and Paul J. Low^{a,*}

^a*Chemistry Department, Durham University Science Laboratories, South Road, Durham, DH1 3LE, U.K. E-mail: m.a.fox@durham.ac.uk, p.j.low@durham.ac.uk*

^b*Department of Chemistry IFM, University of Torino, via P. Giuria 7, 10125 Torino, Italy. E-mail: carlo.nervi@unito.it*

Abstract

The influence of aryl ring substituents X (F, OMe, NMe₂, NH₂, OH and O⁻) on the physical and electronic structure of the *ortho*-carborane cage in a series of C,C'-diaryl-*ortho*-carboranes, 1-(4-XC₆H₄)-2-Ph-1,2-C₂B₁₀H₁₀ has been investigated by crystallographic, spectroscopic (NMR, UV-Vis), electrochemical and computational methods. The cage C1-C2 bond lengths in this carborane series show small variations with the electron-donating strength of the substituent X, but there is no evidence of a fully evolved quinoid form within the aryl substituents in the ground state. In the ¹¹B and ¹³C NMR spectra the 'antipodal' shift at B12, and the C1 shift correlate with the Hammett σ_p value of the substituent, X. The UV-Visible absorption spectra of the cluster compounds show marked differences when compared with the spectra of the analogous substituted benzenes. These spectroscopic differences are attributed to variation in contributions from the cage orbitals to the unoccupied/virtual orbitals involved in the transitions responsible for the observed absorption bands. Electrochemical studies (cyclic voltammetry) carried out on the diarylcarborane series reveal that one-electron reduction takes place at the cage in every case with the voltage required for reduction of the cage influenced by the electron-donating strength of the substituent X, affording a large series of carborane radicals with formal [2n+3] electron counts.

Introduction

The chemistry of carborane cluster compounds has been extensively investigated over many years, and yet exploration of the synthetic, structural and electronic properties of these compounds continue to provide new insights and opportunities for further development. For example, it has long been known that despite their remarkable thermal and oxidative stability, the *closo*-icosahedral carboranes $C_2B_{10}H_{12}$ (most notably the 1,2-*ortho* isomers) are susceptible to attack by Lewis bases which remove BH units.¹ The *nido*-icosahedral fragment dianions $[C_2B_9H_{11}]^{2-}$ that result from these “decapitation” reactions feature pentagonal open faces, which can be coordinated to metal centres and regenerate 12-vertex metallacarborane deltahedra, which have fascinating analogies with both borane clusters and half-sandwich metal complexes.²

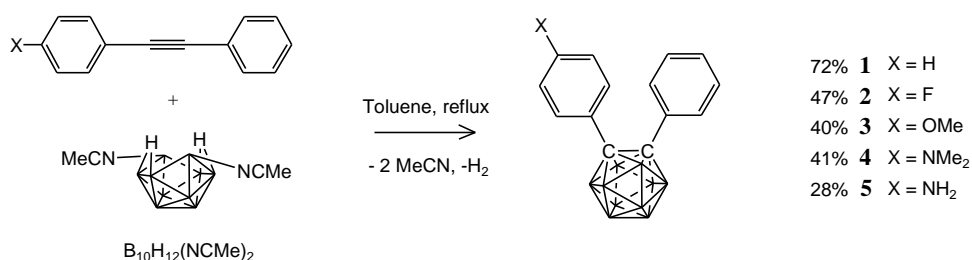
The 12-vertex *closo-ortho*-carborane C_2B_{10} cage is also remarkably structurally flexible in its own right. The cage C1-C2 bond is sensitive to the nature of the groups bonded to the carbon centres, and can be elongated by the attachment of π -donor substituents to one or both of the cage carbon atoms. In extreme cases the cage acquires a tetragonal open face.^{3,4} For example, our work on substituted derivatives of phenyl-*ortho*-carborane, PhCbX (where PhCb = 2-Ph-1,2- $C_2B_{10}H_{10}$ and X = H, F, NH₂, NH⁻, OH, O⁻, bonded at cage carbon C1) has shown that the cage C(1)-C(2) distance increases in relation to the π -donor properties of the substituent, from 1.649(2) Å (X = H) to 2.001(3) Å (X = O⁻).⁴ Structural changes of this magnitude and precision make the *ortho*-carborane residue a very sensitive probe of the π -donor properties of substituents.

It has long been known that two-electron reduction of icosahedral carboranes generates *nido*-dianions $[C_2B_{10}H_{12}]^{2-}$,⁵ which can be used as precursors to 13-vertex metallacarboranes,⁶ with electrochemical studies of diphenyl-*ortho*-carborane PhCbPh (**1**) in acetonitrile or DMSO revealing two sequential quasi-reversible 1e reduction processes.^{7,8} Based on computational (B3LYP/6-31G*) studies, the geometry of the thermodynamically stable radical anion [**1**]⁻ is thought to contain a long cage C1-C2 bond (2.38 Å), arising from the contribution of the additional electron to the cluster skeletal electron count.⁸

We were interested in further exploring the influence of π -donor substituent effects on the physical and electronic structure of the *closo-ortho*-carborane cage. To this end, a series of *ortho*-carborane derivatives $\text{PhCbC}_6\text{H}_4\text{X}$, where $\text{X} = \text{H}, \text{F}, \text{OMe}, \text{NMe}_2, \text{NH}_2$ and OH , were prepared and structurally characterised. The phenyl group at the carbon centre C2 helps resolve possible CH/BH disorder problems,^{4,9,10} and provides an internal structural and spectroscopic reference, thereby gauging the effect of the substituent X of the *para*- XC_6H_4 group at C1 accurately. Within the series, electrochemical measurements have been used to demonstrate that $[2n+3]$ cluster radicals are not unique to the framework of **1**. In this contribution we report structural, spectroscopic, electrochemical and computational work that reveals a degree of interaction between the carborane cage and the remote substituent, X, mediated by the intervening phenylene ring.

Results and Discussion

The parent diphenyl-*ortho*-carborane **1** and the C,C'-diaryl-*ortho*-carboranes, $\text{PhCbC}_6\text{H}_4\text{X}$ [$\text{X} = \text{F}$ (**2**), OMe (**3**), NMe_2 (**4**), NH_2 (**5**)] were prepared from reactions of the appropriate diarylethyne with decaborane (Scheme 1).^{11,12,13} The hydroxy derivative $\text{PhCbC}_6\text{H}_4\text{OH}$ **6** was obtained from demethylation of **3**. The sodium salt $\text{Na}[\text{PhCbC}_6\text{H}_4\text{O}]$ **7** was formed as yellow crystals from **6** and NaOH in acetonitrile.



Scheme 1

Structural aspects

The derivatives $\text{PhCbC}_6\text{H}_4\text{X}$ **1-6** were structurally characterised by single crystal X-ray crystallography, and relevant molecular parameters are listed in Table 1. The molecular geometries of **2-6** resemble that of diphenyl-*ortho*-carborane PhCbPh **1** reported earlier at room temperature,⁹ and re-determined in this work at low temperature for consistency. It is remarkable that the structures of **1** and all its derivatives contain more than one independent molecule, viz. two in **1, 2, 4** and **5**,

four in **3** and six in **6**, the asymmetric unit of the latter also containing a half molecule of hexane, which is located at an inversion centre and partially disordered. Generally, only about 8% of molecular crystals have $Z' > 1$,¹⁴ although the proportion is much higher for certain chemical classes, notably monoalcohols^{15,16} (cf. **6**). Persistence of $Z' > 1$ in the present case can be attributed to the shape of the diphenylcarborane moiety, which is awkward for packing yet has certain conformational flexibility brought about by rotation of the phenyl groups.

In each independent molecule of **2**, the p-fluorine substituent is disordered over both phenyl rings (Figure 1). The occupancies of these positions, F(1) and F(2), in molecule A were refined to 93.3(3) and 6.7(3)%, in molecule B to 61.8(3) and 38.2(3)%.

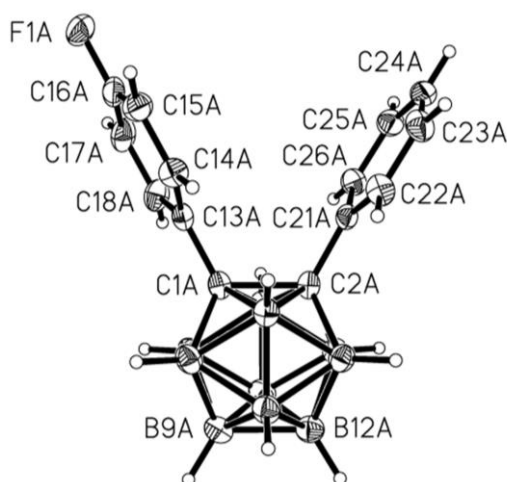


Figure 1. A plot of one unique molecule of **2** (A) showing the important atom labels. The numbering scheme also applies to the structures of **3-6**.

Table 1. Bond distances (Å) and torsion angles (°)

		C(1)-C(2)	θ_1	θ_2	θ_{av}	C(1)-C(13)	C(2)-C(21)	C(16)-X	C(13)-C(14)	C(14)-C(15)	C(15)-C(16)
1^a (H)	A	1.733(4)	2.4	2.3	2	1.500(4)	1.508(5)	-	1.384(5)	1.385(6)	1.363(7)
	B	1.720(4)	9.2	8.0	9	1.494(4)	1.508(4)	-	1.378(5)	1.383(6)	1.364(7)
1 (H)	A	1.730(2)	1.9	4.7	3	1.505(2)	1.509(2)	-	1.392(2)	1.388(2)	1.380(3)
	B	1.722(2)	10.6	8.8	10	1.505(2)	1.505(2)	-	1.389(2)	1.389(2)	1.375(3)
2 (F)	A	1.731(2)	11.6	8.2	10	1.500(2)	1.509(2)	1.359(2) ^b	1.395(3)	1.391(3)	1.371(3)
	B	1.722(2)	15.3	14.3	15	1.502(2)	1.500(2)	1.338(3) ^b	1.397(2)	1.389(3)	1.376(3)
3 (OMe)	A	1.728(2)	14.1	6.0	10	1.498(2)	1.503(2)	1.366(2)	1.395(2)	1.382(2)	1.385(2)
	B	1.730(2)	6.5	4.1	5	1.502(2)	1.508(2)	1.365(2)	1.393(2)	1.382(2)	1.387(2)
	C	1.732(2)	14.5	1.8	8	1.502(2)	1.507(2)	1.368(2)	1.394(2)	1.384(2)	1.388(2)
	D	1.734(2)	8.1	1.6	5	1.499(2)	1.506(2)	1.367(2)	1.396(2)	1.382(2)	1.388(2)
4 (NMe ₂)	A	1.744(3)	6.7	22.3	14.5	1.492(4)	1.502(4)	1.371(3)	1.393(4)	1.382(4)	1.404(4)
	B	1.752(3)	8.6	7.6	8	1.495(3)	1.500(3)	1.376(3)	1.395(2)	1.383(2)	1.393(2)
5 (NH ₂)	A	1.735(2)	22.9	15.9	19	1.498(2)	1.498(2)	1.383(2)	1.395(2)	1.385(2)	1.398(2)
	B	1.748(2)	2.7	11.1	7	1.496(2)	1.505(2)	1.379(2)	1.395(2)	1.383(2)	1.393(2)
6 (OH)	A	1.716(2)	20.3	23.1	22	1.504(2)	1.505(2)	1.373(2)	1.383(2)	1.380(2)	1.373(2)
	B	1.729(2)	4.3	11.7	8	1.503(2)	1.500(2)	1.368(2)	1.382(2)	1.383(3)	1.370(2)
	C	1.718(2)	2.5	9.7	6	1.502(2)	1.501(2)	1.371(2)	1.391(2)	1.387(2)	1.385(2)
	D	1.716(2)	31.3	30.6	31	1.502(2)	1.505(2)	1.370(2)	1.394(2)	1.387(2)	1.387(2)
	E	1.720(2)	23.4	34.1	28.5	1.500(2)	1.506(2)	1.372(2)	1.393(2)	1.388(2)	1.388(2)
	F	1.725(2)	2.3	9.0	6	1.499(2)	1.503(2)	1.369(2)	1.397(2)	1.387(2)	1.390(2)

^a Room temperature, ref. 9; ^b major disordered position;

θ is the average difference between 90 and the moduli of $C_{cage}-C_{cage}-C_{Ph}-C_{Ph}$ torsion angles, i.e. C(1)-C(2)-C(13)-C(14) and C(1)-C(2)-C(13)-C(18) for θ_1 , C(1)-C(2)-C(21)-C(22) and C(1)-C(2)-C(21)-C(26) for θ_2 .

In **3** the methoxy groups are almost coplanar with the phenyl rings to which they are attached; the torsion angle C(15)-C(16)-O(1)-C(19) being $-0.5(2)$, $6.0(2)$, $6.6(2)$ and $-5.6(2)^\circ$ in molecules A, B, C and D, respectively. In **4** the amino group is planar, the sum of C-N-C angles being $359.8(2)^\circ$ in molecule A and $359.0(4)^\circ$ in B. The dihedral angle between the C(19)N(1)C(20) [NMe₂] plane and the benzene ring is 6.1° (A) and 10.4° (B). In **5** the amino group is less planar than in **4**, the sum of bond angles at N(1) being $349(3)^\circ$ in both molecules. Thus, the NH₂ plane makes a dihedral angle of 26° (A) or 34° (B) with the benzene ring, while the p π orbital of C(16) and the lone electron pair of N(1) are eclipsed in molecule A and twisted by ca. 7° in B. Surprisingly there is no strong N-H...N hydrogen bonding in **5**. The NH₂ group of molecule B has one H atom pointing toward the N(1)-C(16) bond rather than the N(1) lone pair of molecule A, and another toward the C(13)-C(14) bond of its equivalent by the transformation (i) $x-1/2, y, 3/2-z$ (Figure 2). For the idealized N-H bond lengths of 1.01 Å, the calculated distances H(2B)...N(1A) 2.48, H(2B)...C(16A) 2.61, H(1B')...C(13A) 2.68 and H(1B')...C(14A) 2.75 Å are somewhat shorter than the sums of van der Waals radii, H...N 2.74 and H...C 2.88 Å. The amino hydrogens of molecule A form only H...H contacts with carborane hydrogens, and those not shorter (2.20-2.26 Å) than twice the van der Waals radius of H (2.2 Å).

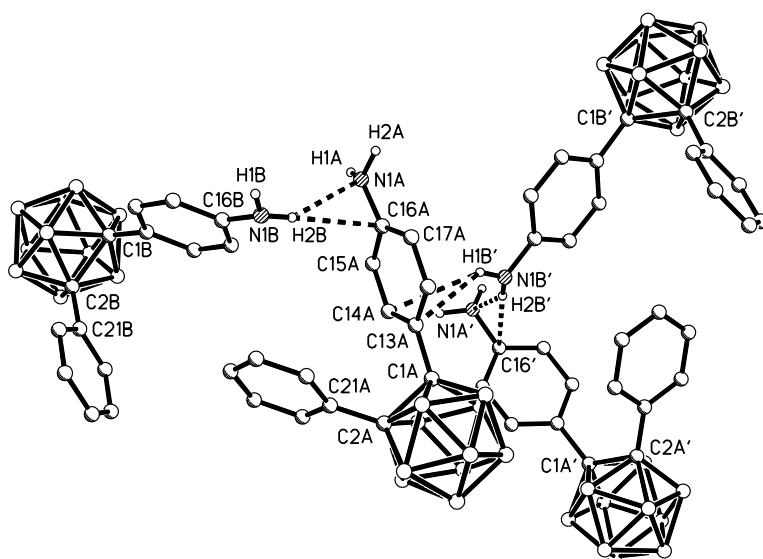


Figure 2. An illustration showing the intermolecular interactions between the two independent molecules in the crystal of **5**.

The molecules of **6** are hydrogen-bonded into two non-equivalent centrosymmetric hexamers, viz. $ABCA^iB^iC^i$ and $DEFD^{ii}E^{ii}F^{ii}$, where symmetry operations are (i) $1-x, -y, -z$ and (ii) $-x, 1-y, -z$. In the $ABCA^iB^iC^i$ cycle all hydroxyl hydrogens are disordered, so that hydrogen bonds can run along the ring in either direction with equal probability, whereas in the latter hexamer, the hydroxyl H atoms are ordered and the hydrogen bonds are donated in the succession $F \rightarrow E \rightarrow D \rightarrow F^{ii}$, etc. (Figure 3).

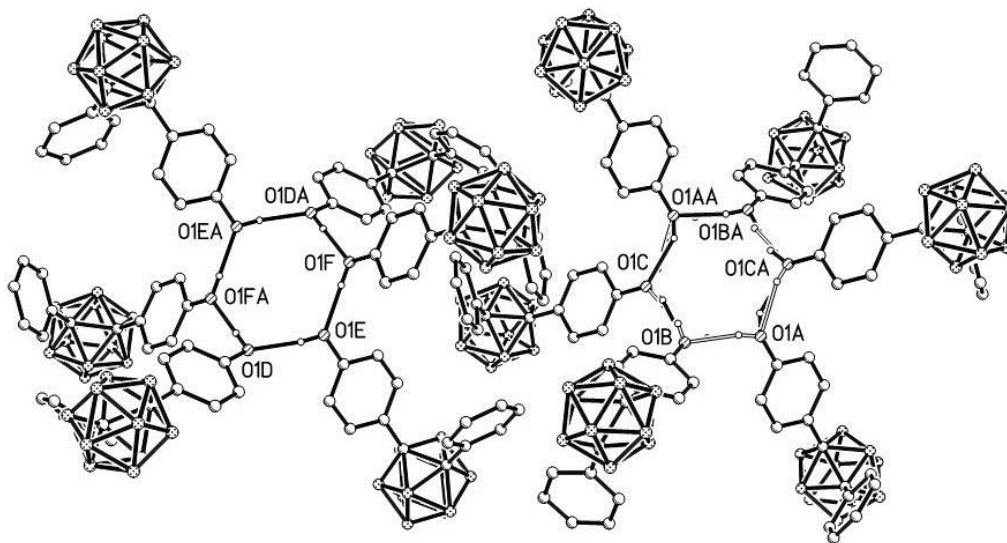


Figure 3. An illustration of the two non-equivalent centrosymmetric hexamers in the crystal of **6**.

Throughout the series **2** - **6** both phenyl rings are orientated roughly perpendicular to the C(phenylene)-C(1)-C(2)-C(phenyl) plane, slightly rotated in the same sense (propeller-like conformation). It is helpful to the discussion to define θ as the average difference between 90 and the moduli of $C_{\text{cage}}-C_{\text{cage}}-C_{\text{Ph}}-C_{\text{Ph}}$ torsion angles, i.e. C(1)-C(2)-C(13)-C(14) and C(1)-C(2)-C(13)-C(18) for θ_1 , C(1)-C(2)-C(21)-C(22) and C(1)-C(2)-C(21)-C(26) for θ_2 .⁹ The range of angles θ is rather small, and generally less than 15° , save for some members of the hydrogen-bonded networks of **6**. Nevertheless, the cage C(1)-C(2) bond is sensitive to aryl group orientations,^{17,18} and the C(1)-C(2) bond length is generally longest when both aryl groups are orientated perpendicular to the C1-C2 vector ($\theta = 0^\circ$) (Table 1) and thereby maximising the interaction between the aryl π -system and the tangential cage carbon p-orbital.^{9,17}

A more significant though still modest variation in the C(1)-C(2) bond length is observed as a function of the electronic character of the substituent X. For example, the length in the parent compound **1** [1.726(2) Å] is shorter than in the NMe₂ derivative **4** [1.744(3), 1.752(3) Å]. The less strongly π -donating groups have more limited influence on the structure of the cage (Table 1), and in any event, the structural variations in response to the substituent are small compared to the changes in C(1)-C(2) bond distances observed when the substituent X is directly bonded to the cage carbon C(1). The C(1)-C(13) and C(2)-C(21) bond lengths in compounds **1-6** are largely insensitive to both the orientation of the phenyl groups and the substituent being ca 1.50 Å in each case.

Very good agreements between the MP2/6-31G* optimised geometry and crystallographically determined structures of **1** have been noted elsewhere.¹⁷ The MP2-optimised geometries of **2-6** reveal the same trends in the cage C1-C2 bond lengths as observed crystallographically i.e. the cage C1-C2 bond length increases with increasing electron-donating effect of X. The optimised geometry of the salt [PhCbC₆H₄O]⁻ Na⁺ **7** contains a C1-C2 bond length of 1.732 Å, which is *ca* 0.02 Å longer than those of MP2-optimised geometries of **1-6** but much shorter than the C1-C2 bond length of 1.913 Å in the MP2-optimised geometry of [PhCbO]⁻ Na⁺ reported previously.⁴ There is no significant quinonoidal character in the substituted ring systems in either the experimental or computational models, and in general the bond lengths within the C(13)-C(18) ring are comparable with those of the analogous substituted benzenes determined experimentally¹⁹ or by computation at the MP2/6-31G* level of theory.

Table 2. Comparison between observed and calculated (in italics) bond distances (Å) and θ_{av} angles (°).

	C(1)-C(2)	θ_{av}	C1-C2 ^a	θ_{av} ^a	C1-C2 ^b	θ_{av} ^b
1 (H)	1.726(2)	7	<i>1.705</i>	<i>17.4</i>	<i>1.718</i>	<i>3.5</i>
2 (F)	1.727(2)	12	<i>1.707</i>	<i>17.0</i>	<i>1.719</i>	<i>3.5</i>
6 (OH)	1.721(2)	17	<i>1.711</i>	<i>16.7</i>	<i>1.723</i>	<i>3.5</i>
3 (OMe)	1.731(2)	7	<i>1.710</i>	<i>17.1</i>	<i>1.723</i>	<i>3.5</i>
5 (NH ₂)	1.741(2)	13	<i>1.714</i>	<i>16.3</i>	<i>1.729</i>	<i>3.5</i>
4 (NMe ₂)	1.748(3)	11	<i>1.715</i>	<i>16.4</i>	<i>1.731</i>	<i>3.5</i>
7 (ONa)			<i>1.732</i>	<i>18.0</i>	<i>1.770</i>	<i>3.5</i>

^a fully optimised ^b optimised with fixed aryl orientations

Spectroscopic aspects

NMR Spectroscopy

Within the PhCbC₆H₄X series the increasing electron-donating effect of X causes a relative decrease in the shielding of the C1 nuclei (Table 3).²⁰ In the ¹¹B NMR data for these series the boron atom B12 antipodal to C1 is most influenced, becoming more shielded when X = NH₂ and NMe₂. These variations in the B12 chemical shift are examples of the ‘antipodal’ effect,²¹ where the substituent at one vertex atom of a cage has a remarkable influence on the chemical shift of the vertex atom directly opposite. In contrast, the chemical shifts of C2 and B9 are relatively insensitive to the nature of X.

Table 3. Observed (in ppm, CDCl₃) and calculated values (in italics) of ¹³C NMR shifts for the cage carbons C1 and C2 and ¹¹B NMR shifts for the antipodal borons B9 and B12 in the PhCbC₆H₄X series. Hammett σ_p values are listed in order for comparison.

X	C1	<i>C1</i>	C2	<i>C2</i>	ΔC	<i>ΔC</i>	B12	<i>B12</i>	B9	<i>B9</i>	ΔB	<i>ΔB</i>	σ_p
F (2)	84.3	<i>84.3</i>	85.3	<i>85.7</i>	-1.0	<i>-1.4</i>	-2.3	<i>-1.5</i>	-2.3	<i>-1.5</i>	0.0	<i>0.0</i>	+0.06
H (1)	85.2	<i>85.7</i>	85.2	<i>85.7</i>	0.0	<i>0.0</i>	-2.4	<i>-1.6</i>	-2.4	<i>-1.6</i>	0.0	<i>0.0</i>	0.00
OMe (3)	85.7	<i>85.1</i>	85.4	<i>86.1</i>	+0.3	<i>+1.0</i>	-2.6	<i>-2.0</i>	-2.6	<i>-1.5</i>	0.0	<i>-0.5</i>	-0.27
OH (6)	85.4	<i>85.5</i>	85.4	<i>85.6</i>	0.0	<i>-0.1</i>	-2.6	<i>-2.0</i>	-2.6	<i>-1.5</i>	0.0	<i>-0.5</i>	-0.37
NH ₂ (5)	86.8	<i>86.7</i>	85.6	<i>85.4</i>	+1.2	<i>+1.3</i>	-3.1	<i>-2.4</i>	-2.6	<i>-1.6</i>	-0.5	<i>-0.8</i>	-0.66
NMe ₂ (4)	87.7	<i>87.5</i>	85.8	<i>85.4</i>	+2.9	<i>+2.1</i>	-3.3	<i>-2.5</i>	-2.6	<i>-1.5</i>	-0.7	<i>-1.0</i>	-0.83
ONa ⁺ (7)	89.9	<i>91.5</i>	85.7	<i>85.2</i>	+4.2	<i>+6.3</i>	-4.1	<i>-4.1</i>	-2.5	<i>-1.8</i>	-1.6	<i>-2.4</i>	

Calculated boron and carbon NMR shifts at the B3LYP/6-311G* level of theory on these MP2-optimised systems also show the same trends as the observed chemical shifts where X influences the frequency of the C1 and B12 resonances but leave C2 and B9 shifts largely unaffected. Calculated NMR values generated from the optimised geometry of the salt $\text{Na}^+[\text{PhCbC}_6\text{H}_4\text{O}]^-$ **7** gave very good agreement with observed data for the sodium salt. An approximately linear relationship exists between the Hammett σ_p values of the substituents and both the ^{13}C chemical shifts of C1 and the ^{11}B NMR chemical shift of B12. This observation lends additional support to the idea that the variation in the observed chemical shifts of these nuclei is attributable to the electronic character of the substituent, with the polarisation of the X-C bond being transmitted to the antipodal boron centre.²²

Electronic Structure Calculations

Electronic structure calculations were carried out on the MP2-optimised geometries of $\text{PhCbC}_6\text{H}_4\text{X}$ **1-6** and the benzene analogues, PhX , at the B3LYP/6-311G* level of theory. Whilst the HOMO in **1** is essentially comprised of the phenyl ring π orbitals, the LUMO features an important contribution from the atoms of the cage (29%) in addition to the phenyl π^* system. These frontier orbitals are stabilised relative to the analogous orbitals in benzene, as expected following the introduction of the electron-withdrawing carborane group (Figure 4). The stabilising effect of the orbital contribution of the cage to the LUMO results in smaller HOMO-LUMO gaps in the cluster systems than in the benzene derivatives (Figure 5).

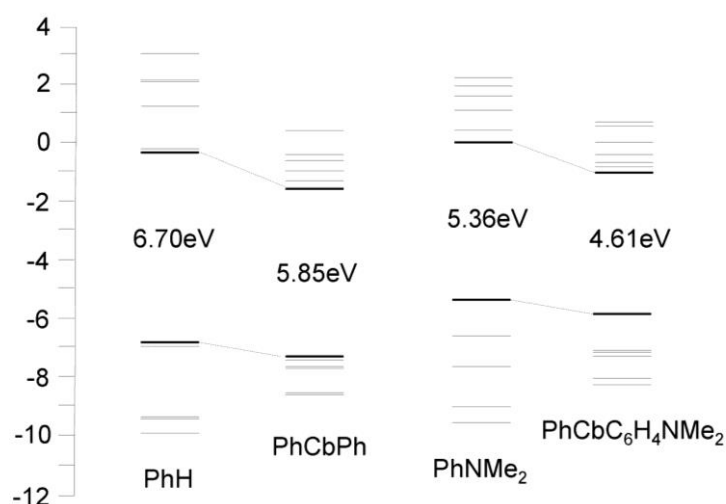


Figure 4. MO diagram for $\text{PhCbC}_6\text{H}_4\text{X}$ and PhX ($\text{X} = \text{H}, \text{NMe}_2$).

The N,N-dimethylamino substituted compound **4** provides an example with which to discuss the influence of the substituents on the electronic structure of 1,2-diphenyl *ortho* carboranes relative to the parent system **1**. The introduction of the electron-donating NMe₂ group in **4** results in a separation of the HOMO which has appreciable N,N-dimethylamino character, from the other occupied orbitals. In contrast, the HOMO of **1** lies closer to the other occupied orbitals. As indicated above, the LUMO and other closely lying unoccupied orbitals have appreciable cage carbon and phenyl ring character (Figure 5). However, whilst the LUMO is evenly distributed over both phenyl rings in **1**, it is more heavily localised on the unsubstituted ring in **4**, as might be expected following the introduction of the strongly electron donating NMe₂ group. The orbitals in the other donor substituted carboranes (**3**, **5** and **6**) are similar to those of **4** (Figure 4). In contrast, the inductively electron withdrawing F group in **2** has little effect on the electronic structure and the frontier orbitals of this species are similar to those of **1**.

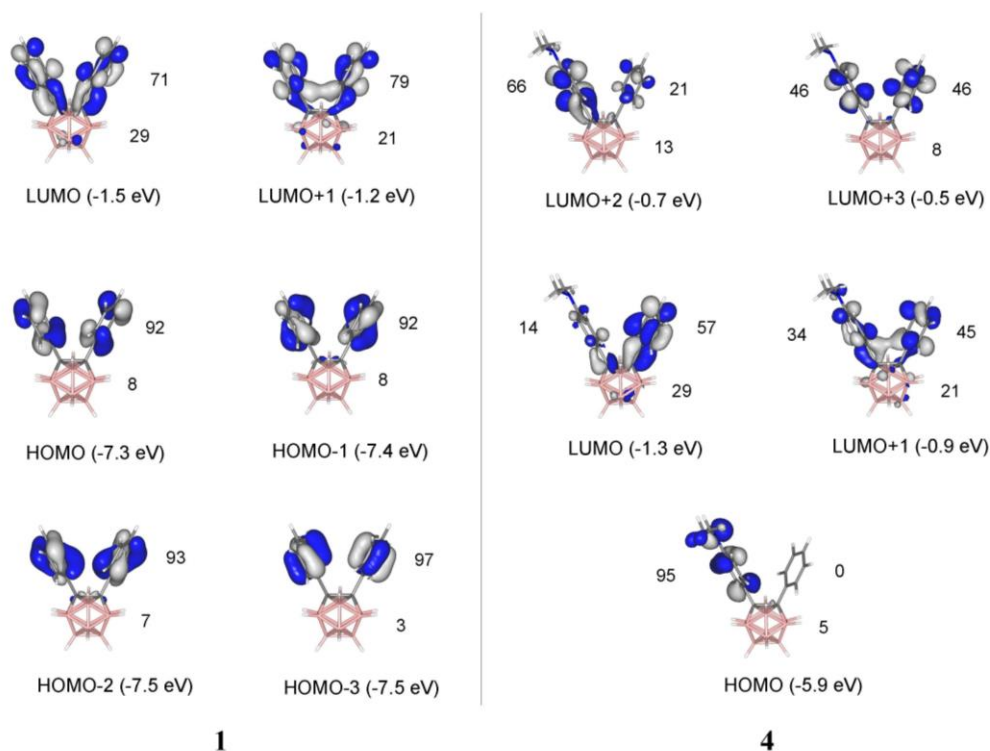


Figure 5. Selected frontier molecular orbitals for PhCbPh **1** and PhCbC₆H₄NMe₂ **4**. Numbers without parentheses represent orbital contributions from phenyl groups and cage.

UV-Visible Spectroscopy

The influence of the carborane cage contribution to the low-lying unoccupied orbitals in **1** – **6** should be apparent in the electronic absorption spectra of these compounds in comparison with the spectra of the analogous substituted benzenes. Electronic absorption spectra were recorded for the carborane series **1-6** from tetrahydrofuran solutions (Figure 6, Table 4). To aid in the assignment of the observed transitions, TD-DFT computations were carried out on MP2-optimised geometries of these systems at the B3LYP/6-311G* level of theory. UV-Visible spectra from the substituted benzenes PhX, also recorded as tetrahydrofuran solutions, are depicted for comparison (Figure 6).

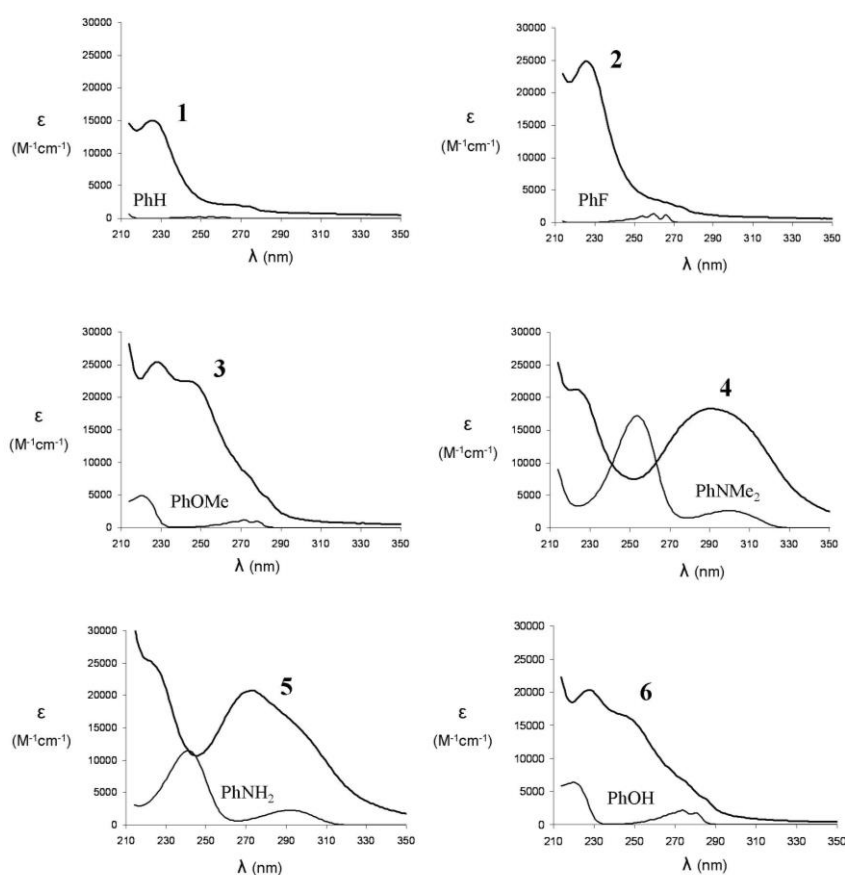


Figure 6. UV-Vis spectra for carboranes **1-6** and their benzene analogues in THF.

Table 4. UV-Visible data [λ_{\max} / nm (ϵ_{\max} / $\text{M}^{-1}\text{cm}^{-1}$)] for PhCbC₆H₄X **1-6** in THF with assignments based on TD-DFT computations.

1 (X = H)		2 (X = F)		3 (X = OMe)	
$\lambda(\epsilon)$	assignment	$\lambda(\epsilon)$	assignment	$\lambda(\epsilon)$	assignment
225 (15000)	HOMO-n \rightarrow LUMO (n = 0-3)	226 (24800)	HOMO-n \rightarrow LUMO (n = 0-3)	228 (25500)	HOMO-1 \rightarrow LUMO
261 (2100)		261 (3500)		248 (22500)	HOMO \rightarrow LUMO+1
267 (2100)		267 (2900)		272 (10000, sh)	
274 (1800)		274 (2400)		276 (8300)	
				284 (4300)	

4 (X = NMe ₂)		5 (X = NH ₂)		6 (X = OH)	
$\lambda(\epsilon)$	assignment	$\lambda(\epsilon)$	assignment	$\lambda(\epsilon)$	assignment
223 (21200)	HOMO-2 \rightarrow LUMO	223 (25300)	HOMO-2 \rightarrow LUMO	227 (20400)	HOMO-1 \rightarrow LUMO
291 (18300)	HOMO \rightarrow LUMO+1 HOMO \rightarrow LUMO+3	273 (20800)	HOMO \rightarrow LUMO+1 HOMO \rightarrow LUMO+3	244 (16500)	HOMO \rightarrow LUMO+1
305 (12000, sh)	HOMO \rightarrow LUMO	293 (16500, sh)	HOMO \rightarrow LUMO	273 (9100, sh)	
				279 (6600)	
				288 (4200)	

The parent compound **1** shows a strong band at 220 nm and very weak, vibrationally structured bands at 261, 267 and 274 nm,²³ similar to those found in benzene.²⁴ On the basis of the TD DFT calculations, the HOMO-*n* (*n* = 0 - 3) and LUMO (Figure 5) are most heavily involved in the most intense absorption band, which approximates the phenyl-localised π - π^* transitions. The spectrum of the fluoro compound **2** displayed a similar spectroscopic profile, confirming that the electron withdrawing F group has little effect on the electronic structure.

The UV-Visible spectra of compounds **3-6** with electron-donating substituents are generally red-shifted and of greater intensities than the benzene analogues PhX (Figure 6). TD-DFT computations on these compounds **3-6** show that the bands correspond to transitions from the π -orbitals localised on the rings with electron-donating substituent X ('donor') to the π^* orbitals localised on the unsubstituted phenyl rings ('acceptor').

Electrochemical studies

The electrochemical behaviours of the diaryl-*ortho*-carboranes (**1-6**) were studied by cyclic voltammetry (CV) and square wave voltammetry (SWV) on a glassy carbon (GC) electrode in acetonitrile with 0.1 M tetrabutylammonium hexafluorophosphate (TBAPF₆) as supporting electrolyte. Table 5 reports the half-wave potentials ($E_{1/2}$), calculated as the mean between cathodic and anodic peak potentials, and the cathodic to anodic peak separation, ΔE_p , in MeCN at 0.2 V/s for the diaryl carboranes **1-6**. The CV and SWV data of compounds **1-6** show two sequential quasi-reversible 1e reduction processes. As the scan rate is increased, the cathodic-to-anodic peak separation (ΔE_p) of the first redox process (0/-1) increases more than the ΔE_p of the second reduction (-1/-2), as shown in Figure 7 for compounds **1** and **5** for illustrative purposes. It is therefore likely that the heterogeneous electron transfer rate of the second reduction is faster than the first.

Table 5. The electrochemical response of **1-6** in MeCN at 0.2 V/s, listed in order of the electron-donating ability of the substituent X in 1-(4-XC₆H₄)-2-Ph-1,2-C₂B₁₀H₁₀.

X		E_p^c (V)	E_p^a (V)	$E_{1/2}$ (V)	ΔE_p (mV)
F	2	-1.61	-1.48	-1.53	125
		-1.72	-1.65	-1.69	71
H	1	-1.63	-1.50	-1.56	123
		-1.76	-1.68	-1.73	75
OH	6	-1.66	-1.57	-1.61	90
		-1.78	-1.71	-1.75	70
OMe	3	-1.65	-1.55	-1.60	98
		-1.78	-1.71	-1.75	72
NH ₂	5	-1.71	-1.61	-1.65	95
		-1.82	-1.75	-1.79	74
NMe ₂	4	-1.70	-1.62	-1.66	84
		-1.82	-1.75	-1.79	72

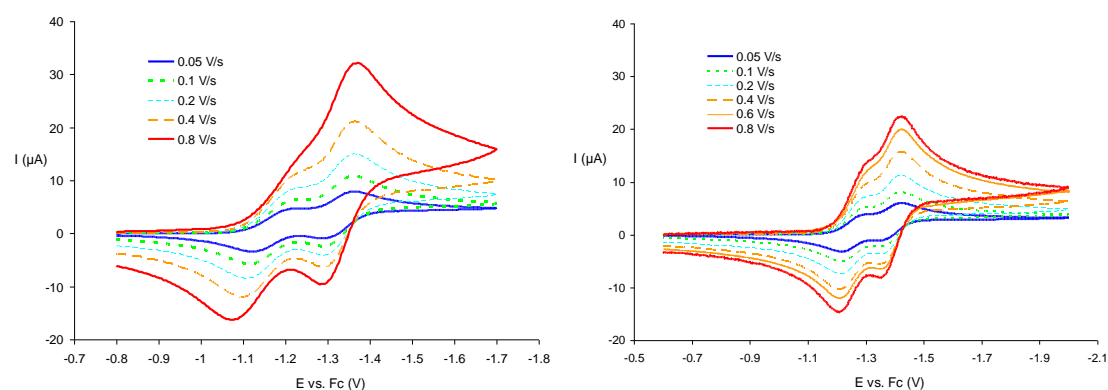


Figure 7. Cyclic Voltammograms of 1,2-diphenyl-*ortho*-carborane (**1**) (left) and 1-(4-aminophenyl)-2-phenyl-*ortho*-carborane (**5**) (right) in acetonitrile at GC electrode with various scan rates.

Unsurprisingly, the reduction potentials of **1-6** shift to more negative values as the substituent X becomes more electron donating, for example, the $E_{1/2}$ value of **4** (X = NMe₂) is *ca* 100 mV more negative than that of **1** (X = H). Digital simulations of the experimental voltammograms were successfully achieved using a simple EE electrochemical mechanism; thermodynamic and kinetic parameters are summarised in Table 6, and illustrated, for example, for compound **1** (Figure 8). Crucially, the observation of two distinct reduction processes for each member of the series **1 – 6** indicates that the thermodynamically stable radical anions, which possess $[2n+3]$ skeletal electron counts, are a general feature of C,C'-diaryl-*ortho*-carboranes.^{8,25}

Table 6. Thermodynamic and kinetic parameters for 1-(4-XC₆H₄)-2-Ph-1,2-C₂B₁₀H₁₀ **1-6** in acetonitrile based on the simple EE mechanism

X		$k^0(0/-1)$ (cm/s)	$k^0(-1/-2)$ (cm/s)	$\alpha(0/-1)$	$\alpha(-1/-2)$
H	1	$4.0 \cdot 10^{-3}$	$3.8 \cdot 10^{-2}$	0.4	0.35
F	2	$6.0 \cdot 10^{-3}$	$4.0 \cdot 10^{-2}$	0.35	0.3
OMe	3	$1.2 \cdot 10^{-2}$	$5.0 \cdot 10^{-2}$	0.4	0.4
NMe ₂	4	$2.0 \cdot 10^{-2}$	$1.0 \cdot 10^{-1}$	0.4	0.3
NH ₂	5	$1.2 \cdot 10^{-2}$	$1.1 \cdot 10^{-1}$	0.4	0.4
OH	6	$2.2 \cdot 10^{-2}$	$1.6 \cdot 10^{-1}$	0.7	0.4

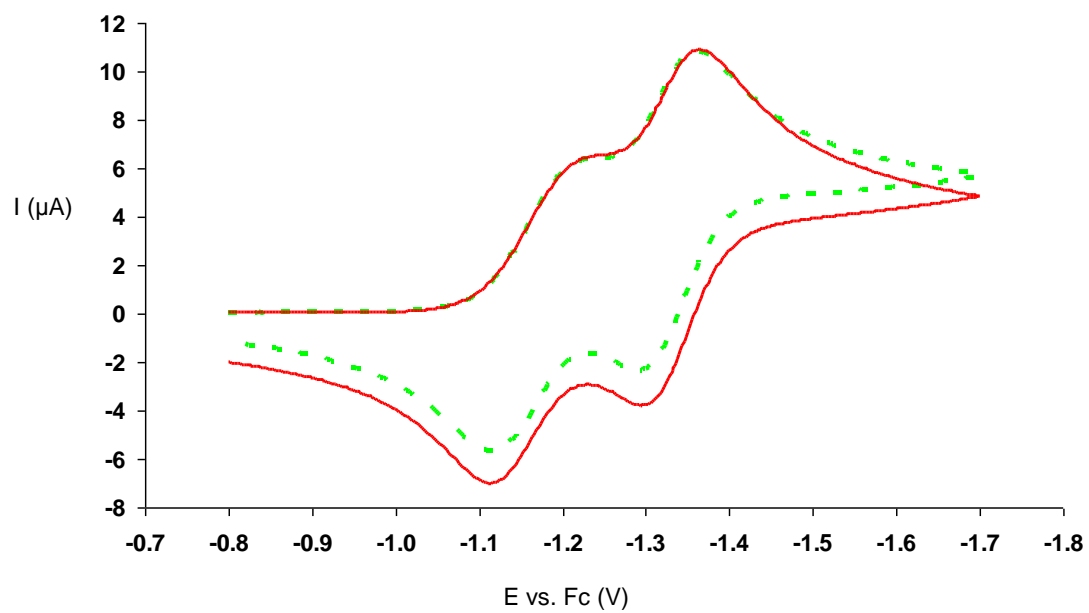


Figure 8. Experimental (green) and simulated (red) CV at 0.1 V/s of 1,2-diphenyl-*ortho*-carborane (**1**) in acetonitrile.

Conclusions

X-ray crystallographic studies for six derivatives PhCbC₆H₄X (X = H, F, OH, OMe, NH₂, NMe₂) **1-6** show small variations in the intra-cage C(1)-C(2) bond lengths with the electronic nature of X, elongating when X is electron-releasing. These variations are much less pronounced than variations in compounds 1-X-2-Ph-1,2-C₂B₁₀H₁₀ studied earlier.⁴ It is remarkable that all crystals of the six carboranes studied here have $Z' > 1$ i.e. more than one independent molecule. Boron-11 NMR data on seven derivatives, 1-(4-XC₆H₄)-2-Ph-1,2-C₂B₁₀H₁₀ (X = H, F, OMe, NMe₂, NH₂, OH, O⁻), corroborate the concept of an electronic effect of the substituent on the cage with the substituent X giving rise to variations in the antipodal boron (B12) chemical shift which correlate well with the electron-donating ability (Hammett σ_p values) of the substituent. The major bands observed in the UV-Vis spectra of the PhCbC₆H₄X series **1-6** (X = H, F, OMe, NMe₂, NH₂ and OH) are red-shifted by the cluster when compared to PhX ring systems, as whilst the electron-withdrawing properties of the carborane cage contribute somewhat to the stabilisation of the HOMO, the carborane contribution to the low-lying unoccupied orbitals involved in these transitions is more significant.

These structural and spectroscopic studies on compounds of general structure 1-(4-XC₆H₄)-2-Ph-1,2-C₂B₁₀H₁₀ have provided evidence of mixing of electronic character between the substituent X and the carborane cage through the intervening phenylene link, which could be interpreted in terms of “electronic communication” between the cage and substituent. Cyclovoltammetric studies also support the notion of interaction between the cage and the group X, with the reduction potentials of the cage tracking the electronic nature of X. These electrochemical studies also provide experimental evidence for the generality of cluster radical anions with $[2n+3]$ skeletal electron counts.

Acknowledgements We thank the EPSRC and Regione Piemonte for generous financial support and the University of Durham High Performance Computing centre for computing facilities.

Experimental Section

All reactions were conducted under dry nitrogen unless otherwise stated. Toluene was dried over sodium metal and distilled prior to use. Pyridine was dried and purified by distillation after standing over KOH. Elemental carbon, hydrogen and nitrogen analyses were performed using Exeter Analytical CE-440 or Carlo Erba Strumentazione EA Model 1106 instruments. Mass spectra (MS) were recorded on a VG Micromass 7070E instrument under E.I conditions (EI) at 70 eV. Values of M show the isotope range $^{10}\text{B}_n$ to $^{11}\text{B}_n$ including a ^{13}C contribution if observed. NMR spectra were measured using Varian Unity-300 (^1H , ^{11}B , ^{13}C), Bruker AM250 (^1H , ^{13}C), Bruker Avance 400 (^1H , ^{11}B , ^{13}C) and/or Varian Inova 500 (^1H , ^{11}B) instruments. All chemical shifts are reported in δ (ppm) and coupling constants in Hz. ^1H NMR spectra were referenced to residual protio impurity in the solvent (CDCl_3 , 7.26 ppm; CD_3CN , 1.95 ppm). ^{13}C NMR spectra were referenced to the solvent resonance (CDCl_3 , 77.0 ppm; CD_3CN , 118.3 ppm). ^{11}B NMR spectra were referenced to external $\text{Et}_2\text{O}\cdot\text{BF}_3$, $\delta = 0.0$ ppm. UV-Visible spectra were recorded in THF solutions with 2 mm pathlength UV cells on a Perkin Elmer Lambda 900 UV-Vis-NIR spectrometer.

Phenylethynylcopper, $\text{PhC}\equiv\text{CCu}$, and 6,9-bis(acetonitrile)decaborane, $\text{B}_{10}\text{H}_{12}(\text{NCMe})_2$, were prepared as previously described.²⁶ The diarylacetylenes, 4- $\text{XC}_6\text{H}_4\text{C}\equiv\text{CPh}$, were synthesised from phenylethynylcopper and the appropriate aryl iodide in pyridine using the literature method described for methyl 4-phenylethynylbenzoate.²⁶ The isolated yields obtained for the diarylethyne where X = F, OMe, NMe₂ and NO₂ were 64, 67, 40 and 70% respectively. Compound **1** was synthesised from diphenylethyne and $\text{B}_{10}\text{H}_{12}(\text{NCMe})_2$ in 72% yield using the literature method described for a related diaryl carborane $\text{PhCbC}_6\text{H}_4\text{CO}_2\text{Me}$.²⁶

For cyclovoltammetric studies, acetonitrile was distilled over calcium hydride just before use. Tetrabutylammonium hexafluorophosphate (Bu_4NPF_6) was obtained as metathesis reaction between KPF_6 (Fluka) and tetrabutylammonium iodide (Aldrich), re-crystallized three times from 95% ethanol and dried in vacuum oven at 110°C overnight. Electrochemistry was performed in a three-electrode cell using a potentiostat AMEL 7050 and an EG&G PAR 273 electrochemical analyser, both connected to a PC. The reference electrode was 3M KCl Calomel Electrode, the

auxiliary electrode a platinum wire and the working electrode a glassy carbon (GC). Positive feedback iR compensation was applied routinely. All measurements were carried out under Ar in anhydrous deoxygenated solvents. Ferrocene (F_c) was used as internal standard, and potentials are reported against the $F_c(0/+1)$ redox couple, that in our conditions is $E^\circ(0/+1) = 0.395$ V.

Syntheses

Synthesis of 1-(4- FC_6H_4)-2-Ph-1,2- $C_2B_{10}H_{10}$, **2**

A stirred slurry of $B_{10}H_{12}(NCMe)_2$ (1.58 g, 7.8 mmol) in toluene (25 ml) was treated dropwise with a solution of 4- $FC_6H_4C\equiv CPh$ (1.35 g, 7.8 mmol) in toluene (20 ml). The mixture was heated at reflux for 18h, giving an orange-red solution. Removal of the solvent *in vacuo* afforded an orange solid. The solid was treated with MeOH (30 ml) and left to stir overnight to destroy any unreacted decaborane. The solvent was removed and the residue extracted with hexane. The hexane extracts were filtered, and the filtrate cooled (-30 °C) to afford large colourless crystals (1.15 g, 47%) of the fluoro compound **2**. M.p. 136-7°C. Found: C, 52.9, H, 6.6 % $C_{14}H_{19}B_{10}F$ requires C, 53.5, H, 6.1 %. MS (EI^+ , m/z): $[M]^+$ 309-316; observed 314 (100). IR (KBr disc, cm^{-1}): 3060w (aryl CH); 2643-2547s (BH); 1608s, 1510s, 1247s, 1168s, 840s, 687s. $^1H\{^{11}B\}$ NMR ($CDCl_3$): δ 7.41 (m, 4H, *ortho* and *ortho'* CH); 7.24 (t, 1H, J_{HH} 7.1, *para'* CH); 7.16 (dd, 2H, $J_{HH} \sim 7.5$, *meta'* CH); 6.82 (dd, 2H, J_{HH} 8.8, J_{HF} 8.4, *meta* CH); 3.22 (s, 2H, H3, 6); 2.55 (s, 6H, H4,5,7,11,9,12); 2.36 (s, 2H, H8,10). $^{11}B\{^1H\}$ NMR ($CDCl_3$): δ -2.3 (s, 2B, B9,12); -9.1 (s, 4B, B4,5,7,11); -10.3 (s, 2B, B8,10); -11.0 (s, 2B, B3,6). $^{13}C\{^1H\}$ NMR ($CDCl_3$): δ 163.0 (d, J_{CF} 255, *para*-CF); 132.9 (d, J_{CF} 9, *ortho*-CH); 130.8 (s, *ortho'*-CH); 130.7 (s, *ipso'*-CH); 130.6 (s, *para'*-CH); 128.6 (s, *meta'*-CH); 127.0 (d, J_{CF} 3, *ipso*-CH); 115.3 (d, J_{CF} 22, *meta*-CH); 85.3 (s, carborane C2); 84.3 (s, carborane C1).

Synthesis of 1-(4-MeOC $_6$ H $_4$)-2-Ph-1,2- $C_2B_{10}H_{10}$, **3**

A solution of 4-MeOC $_6$ H $_4C\equiv CPh$ (10.3 g, 0.05 mol) in toluene (60 ml) was added to a stirred slurry of $B_{10}H_{12}(NCMe)_2$ (10.1 g, 0.05 mol) in toluene (60 ml). The mixture was heated at reflux point for 24 h, during which time hydrogen was evolved and the solution became dark red in colour. After allowing the reaction mixture to cool to 20°C, the solution was diluted with MeOH (60 ml) MeOH to destroy any unreacted

decaborane. The solvents were removed *in vacuo* and the solid residue which was obtained crushed into a powder. This solid was subjected to Soxhlet extraction with hexane (80 ml) for 24h. The crystals (6.4 g, 40 %), formed after cooling and slow evaporation of the hexane extract, were identified as compound **3**.¹³ M.p. 101-2°C. Found: C, 55.4, H, 6.6 % C₁₅H₂₂B₁₀O requires C, 55.2, H, 6.8 %. MS (EI⁺, *m/z*): [M]⁺ 320-329; observed 326 (100). IR (KBr disc, cm⁻¹): 3058w (aryl CH); 2933w (methyl CH); 2632-2579s (BH); 1602m, 1508m, 1257s, 1182s, 838m, 687m. ¹H{¹¹B} NMR (CDCl₃) δ 7.41 (d, 2H, *J*_{HH} 8.4, *ortho*' CH), 7.33 (d, 2H, *J*_{HH} 9.0, *ortho* CH), 7.24 (t, 1H, *J*_{HH} 7.2, *para*' CH), 7.15 (dd, 2H, *J*_{HH} ~7.6, *meta*' CH), 6.62 (d, 2H, *J*_{HH} 9.2, *meta* CH), 3.71 (s, 3H, CH₃), 3.22 (s, 2H, H_{3,6}), 2.52 (s, 6H, H_{4,5,7,11,9,12}), 2.33 (s, 2H, H_{8,10}). ¹¹B{¹H} NMR (CDCl₃): δ -2.6 (s, 2B, B_{9,12}), -9.1 (s, 4B, B_{4,5,7,11}), -10.6 (s, 2B, B_{8,10}), -11.4 (s, 2B, B_{3,6}). ¹³C{¹H} NMR (CDCl₃): δ 160.8 (s, *para*-CO), 132.0 (s, *ortho*-CH), 130.7 (s, *ortho*'-CH and *ipso*'-CH), 130.1 (s, *para*'-CH), 128.3 (s, *meta*'-CH), 123.0 (s, *ipso*-CH), 113.5 (s, *meta*-CH), 85.7 (s, carborane C1), 85.4 (s, carborane C2).

Synthesis of 1-(4-Me₂NC₆H₄)-2-Ph-1,2-C₂B₁₀H₁₀, **4**

A solution of 4-Me₂NC₆H₄C≡CPh (3.32 g, 0.015 mol) in toluene (40 ml) was added to a stirred slurry of B₁₀H₁₂(NCMe)₂ (3.03 g, 0.015 mol) in toluene (50 ml). The mixture was slowly heated to reflux point, during which time hydrogen gas was evolved and the solution turned red. After heating at reflux point for 26 h, the dark red solution was cooled and diluted with MeOH (40 ml). The solvents were removed *in vacuo*, the solid residue crushed into a powder and extracted with boiling hexane. The combined extracts were allowed to cool and the yellow crystals (2.08 g, 41%) that formed were identified as the desired dimethylamino compound **4**. M.p. 158-9°C. Found: C, 57.0, H, 7.1, N, 3.8 % C₁₄H₂₅B₁₀N requires C, 56.6, H, 7.4, N, 4.1 % MS (EI⁺, *m/z*): [M]⁺ 333-341; observed 339 (100). IR (KBr disc, cm⁻¹): 3074w (aryl CH); 2920w (methyl CH); 2625-2559s (BH); 1614s, 1530m, 1373m, 1203s, 759m, 690m. ¹H{¹¹B} NMR (CDCl₃): δ 7.45 (d, 2H, *J*_{HH} 8.4, *ortho*' CH), 7.24 (d, 2H, *J*_{HH} 8.8, *ortho* CH), 7.23 (t, 1H, *J*_{HH} 7.2, *para*' CH), 7.15 (dd, 2H, *J*_{HH} ~8.0, *meta*' CH), 6.36 (d, 2H, *J*_{HH} 8.8, *meta* CH), 2.87 (s, 6H, CH₃), 3.22 (s, 2H, H_{3,6}), 2.50 (s, 5H, H_{4,5,7,11,9}), 2.39(s, 1H, H₁₂), 2.27 (s, 2H, H_{8,10}). ¹¹B{¹H} NMR (CDCl₃): δ -2.6 (s, 1B, B₉), -3.3 (s, 1B, B₁₂), -9.2 (s, 4B, B_{4,5,7,11}), -10.8 (s, 2B, B_{8,10}), -11.4 (s, 2B,

B3,6). $^{13}\text{C}\{^1\text{H}\}$ NMR (CDCl_3) δ 151.1 (s, *para*-CN), 131.6 (s, *ortho*-CH), 130.7 (s, *ortho'*-CH and *ipso'*-CH), 129.9 (s, *para'*-CH), 128.1 (s, *meta'*-CH), 119.2 (s, *ipso*-CH), 110.0 (s, *meta*-CH), 87.7 (s, carborane C1), 85.8 (s, carborane C2).

Synthesis of 1-(4- $\text{H}_2\text{NC}_6\text{H}_4$)-2-Ph-1,2- $\text{C}_2\text{B}_{10}\text{H}_{10}$, **5**

A suspension of $\text{B}_{10}\text{H}_{12}(\text{NCMe})_2$ (4.04 g, 0.02 mol) in toluene (50 ml) was treated with a solution of 4- $\text{H}_2\text{NC}_6\text{H}_4\text{C}\equiv\text{CPh}$ (2.90 g, 0.015 mol) in toluene (40 ml). On heating the solution to reflux point, gas evolution was apparent, which quickly ceased. The green solution was heated at reflux point for 24 h then cooled, diluted with MeOH (30 ml) and stirred for 12 h. The solvents were removed in *vacuo* and the residue extracted with hexane in a Soxhlet apparatus. The extracts were cooled and allowed to slowly evaporate to give crystals of the amino carborane **5** (1.31 g, 28%).²⁷ M.p.165-6°C (lit.²⁷ 169-170°C). Found: C, 53.9, H, 6.6, N, 3.9 % $\text{C}_{14}\text{H}_{21}\text{B}_{10}\text{N}$ requires C, 54.0, H, 6.8, N, 4.5 % MS (EI^+ , m/z): $[\text{M}]^+$ 305-313; observed 311 (100). IR (KBr disc, cm^{-1}): 3465m(br), 3379m(br) (N-H stretch); 3074w (aryl CH); 2920w (methyl CH); 2625-2559s (BH); 1614s, 1530m, 1373m, 1203s, 759m, 690m. $^1\text{H}\{^{11}\text{B}\}$ NMR (CDCl_3): δ 7.45 (d, 2H, J_{HH} 8.4, *ortho'* CH), 7.24 (d, 2H, J_{HH} 8.8, *ortho* CH), 7.23 (t, 1H, J_{HH} 7.2, *para'* CH), 7.15 (dd, 2H, J_{HH} ~8.0, *meta'* CH), 6.36 (d, 2H, J_{HH} 8.8, *meta* CH), 3.71 (s, 2H, NH_2), 3.21 (s, 2H, H3,6), 2.54 (s, 6H, H4,5,7,11,9,12), 2.32 (s, 2H, H8,10). $^{11}\text{B}\{^1\text{H}\}$ NMR (CDCl_3): δ -2.6 (s, 1B, B9), -3.1 (s, 1B, B12), -9.3 (s, 4B, B4,5,7,11), -10.8 (s, 2B, B8,10), -11.5 (s, 2B, B3,6); $^{13}\text{C}\{^1\text{H}\}$ NMR (CDCl_3): δ 148.0 (s, *para*-CN), 131.8 (s, *ortho*-CH), 130.9 (s, *ipso'*-CH), 130.7 (s, *ortho'*-CH), 130.0 (s, *para'*-CH), 128.5 (s, *meta'*-CH), 120.3 (s, *ipso*-CH), 114.0 (s, *meta*-CH), 86.8 (s, carborane C1), 85.5 (s, carborane C2).

Synthesis of 1-(4- HOC_6H_4)-2-Ph-1,2- $\text{C}_2\text{B}_{10}\text{H}_{10}$, **6**

Dry hydrogen chloride was bubbled through pyridine (8 ml) and the resulting solid heated to 170 °C. After 2h and with the temperature still at 170 °C, 1-(4-MeOC₆H₄)-2-Ph-1,2- $\text{C}_2\text{B}_{10}\text{H}_{10}$ **3** (1.96 g, 6 mmol) of was added and the temperature raised to 200 °C for 3h. The reaction mix was left to cool to give a white solid, of which a large part was dissolved in water to leave a gum-like solid. The undissolved solid was collected

by filtration and dried *in vacuo*, before being dissolved in diethyl ether, dried over MgSO₄ and filtered. The ether was removed *in vacuo* to yield a white solid which was recrystallised from hexane to give large colourless crystals (1.24 g, 66 %) of the hydroxy compound **6**.^{13,28} M.p. 136-7°C. Found: C, 54.0, H, 6.6 % C₁₄H₂₀B₁₀O requires C, 53.9, H, 6.4 %. MS (EI⁺, *m/z*): [M]⁺ 309-314; observed 312 (100). IR (KBr disc, cm⁻¹): 3563s (OH stretch); 3066w (aryl CH); 2642-2552s (BH); 1612s, 1515s, 1279s, 1180s, 1173s, 840m, 693m; ¹H{¹¹B} NMR (CDCl₃): δ 7.42 (d, 2H, *J*_{HH} 8.4, *ortho'* CH), 7.28 (d, 2H, *J*_{HH} 9.0, *ortho* CH), 7.24 (t, 1H, *J*_{HH} 7.2, *para'* CH), 7.14 (dd, 2H, *J*_{HH} ~7.6, *meta'* CH), 6.56 (d, 2H, *J*_{HH} 9.2, *meta* CH), 5.82 (s, 1H, OH), 3.23 (s, 2H, H3, 6), 2.54 (s, 6H, H4,5,7,11,9,12), 2.34 (s, 2H, H8,10); ¹¹B{¹H} NMR (CDCl₃): δ -2.6 (s, 2B, B9,12), -9.1 (s, 4B, B4,5,7,11), -10.6 (s, 2B, B8,10), -11.4 (s, 2B, B3,6); ¹³C{¹H} NMR (CDCl₃): δ 156.8 (s, *para*-CO), 132.2 (s, *ortho*-CH), 130.6 (s, *ortho'*-CH and *ipso'*-CH), 130.0 (s, *para'*-CH), 128.1 (s, *meta'*-CH), 122.9 (s, *ipso*-CH), 115.0 (s, *meta*-CH), 85.4 (s, carborane C1 and C2).

Deprotonation of 1-(4-HOC₆H₄)-2-Ph-1,2-C₂B₁₀H₁₀ **6** to give the sodium salt **7**

A cloudy solution of **6** (100 mg, 0.32 mmol) in acetonitrile (5 ml) was treated with a solution of NaOH (100 mg, 2.5 mmol) in water (1 ml). The solution clarified and turned yellow, and after two hours yellow crystals appeared, which were isolated by filtration and identified as the pentahydrate of the sodium salt **7**. Found: C, 40.0, H, 6.6 % C₁₄H₁₉B₁₀ONa.5H₂O requires C, 39.6, H, 6.8 %. MS (ES⁻, *m/z*): [C₁₄H₁₉B₁₀O]⁻ 309-313; observed 311 (100). IR (KBr disc, cm⁻¹): 3414m(br) (OH stretch), 3066w (aryl CH); 2640-2550s (BH); 1560s, 1499s, 1407s, 1261s, 1178s, 844m, 804m, 691m. ¹H{¹¹B} NMR (CD₃CN): δ 7.56 (d, 2H, *J*_{HH} 8.0, *ortho'* CH); 7.31 (t, 1H, *J*_{HH} 7.2, *para'* CH); 7.22 (dd, 2H, *J*_{HH} ~7.6, *meta'* CH); 7.06 (d, 2H, *J*_{HH} 9.2, *ortho* CH); 6.06 (d, 2H, *J*_{HH} 8.8, *meta* CH); 3.26 (s, 2H, H3, 6); 2.47 (s, 5H, H4,5,7,11,9); 2.32 (s, 1H, H12); 2.17 (s, 2H, H8,10), 1.65 (s, 10H, H₂O). ¹¹B{¹H} NMR (CD₃CN) δ -3.0 (s, 1B, B9), -4.6 (s, 1B, B12), -9.4 (s, 4B, B4,5,7,11), -11.7 (s, 4B, B3,6,8,10). ¹³C{¹H} NMR (CD₃CN): δ 171.2 (s, *para*-CO); 132.1 (s, *ortho*-CH); 131.3 (s, *ipso'*-CH); 130.9 (s, *ortho'*-CH); 130.2 (s, *para'*-CH), 128.3 (s, *meta'*-CH); 118.6 (s, *meta*-CH); 113.3 (s, *ipso*-CH); 91.2 (s, carborane C1); 87.0 (s, carborane C2).

For comparison, NMR data for **6** in CD₃CN follow: ¹H{¹¹B} NMR: δ 7.54 (d, 2H, *ortho'* CH); 7.33 (m, 3H, *ortho* CH and *para'* CH); 7.23 (dd, 2H, *meta'* CH); 6.59 (d,

2H, *meta* CH); 3.31 (s, 2H, H3, 6); 2.47 (s, 6H, H4,5,7,11,9,12); 2.25 (s, 2H, H8,10).
 $^{11}\text{B}\{^1\text{H}\}$ NMR: δ -3.1 (s, 2B, B9,12); -9.3 (s, 4B, B4,5,7,11); -11.2 (s, 4B, B3,6,8,10).
 $^{13}\text{C}\{^1\text{H}\}$ NMR: δ 158.9 (s, *para*-CO); 132.5 (s, *ortho*-CH); 130.9 (s, *ortho'*-CH);
130.5 (s, *para'*-CH and *ipso'*-CH); 128.5 (s, *meta'*-CH); 121.8 (s, *ipso*-CH); 115.0 (s,
meta-CH); 86.7 (s, carborane C1 and C2).

Crystallography

X-ray diffraction experiments were carried out on 3-circle Bruker diffractometers with a SMART 1K or (for **1** and **3**) SMART 6K CCD (for **2** and **4–6**) area detectors, using graphite-monochromated Mo- K_α radiation ($\bar{\lambda}$ =0.71073 Å) and a Cryostream open-flow N₂ cryostat (Oxford Cryosystems). Full sphere of reciprocal space (for **4**, a hemisphere) was covered by 3-4 sets of narrow-frame (0.3°) ω scans, each set with different ϕ angle. The structures were solved by direct methods and refined by full-matrix least squares against F^2 of all data, using SHELXTL software.²⁹ Non-hydrogen atoms were refined in anisotropic approximation. The ordered hydroxyl H atoms in **6**, and amino H atoms in **5** were refined in isotropic approximation, the remaining H atoms were included as riding in idealized positions. Crystal data and experimental details are listed in Table 7. Full crystallographic data, excluding structure factors, have been deposited at the Cambridge Crystallographic Data Centre.

Computations

All *ab initio* computations were carried out with the Gaussian 03 package.³⁰ The geometries discussed here were optimised at the HF/6-31G* and B3LYP/6-31G* levels of theory with no symmetry constraints. Frequency calculations were computed on these optimised geometries at the corresponding levels and shown to have no imaginary frequencies. Optimisation of these geometries were then carried out at the MP2/6-31G* level of theory.

Calculated NMR shifts at the GIAO-B3LYP/6-311G* level were obtained from these MP2-optimized geometries. Theoretical ^{11}B chemical shifts at the GIAO-B3LYP/6-311G*//HF-B3LYP-MP2/6-31G* level were referenced to B₂H₆ (16.6 ppm³¹) and converted to the usual BF₃.OEt₂ scale: $\delta(^{11}\text{B}) = 102.83 - \sigma(^{11}\text{B})$. The ^{13}C and ^1H

chemical shifts were referenced to TMS: $\delta(^{13}\text{C}) = 179.81 - \sigma(^{13}\text{C})$; $\delta(^1\text{H}) = 32.28 - \sigma(^1\text{H})$. Electronic structure and TD-DFT computations at the B3LYP/6-311G* level of theory were carried out on these MP2-optimized geometries.

Table 7. Crystal data and experimental parameters.

Compound	1	2	3	4	5	6
CCDC dep. no.	96srv188	06srv191	06srv190	95srv140	06srv189	01srv183
Empirical formula	C ₁₄ H ₂₀ B ₁₀	C ₁₄ H ₁₉ B ₁₀ F	C ₁₅ H ₂₂ B ₁₀ O	C ₁₆ H ₂₅ B ₁₀ N	C ₁₄ H ₂₁ B ₁₀ N	C ₁₄ H ₂₀ B ₁₀ O · 1/12 C ₆ H ₁₄
Formula weight	296.40	314.39	326.43	339.47	311.42	319.58
T, K	150	120	120	150	120	120
Crystal system	monoclinic	orthorhombic	monoclinic	orthorhombic	orthorhombic	triclinic
Space group (No.)	P2 ₁ /c (#14) ^a	P2 ₁ 2 ₁ 2 ₁ (#19)	P2 ₁ /n (#14)	Pbca (#61)	Pbca (#61)	P-1 (#2)
<i>a</i> , Å	10.783(2)	10.808(1)	11.133(1)	11.840(1)	13.554(2)	12.758(1)
<i>b</i> , Å	24.676(5)	11.249(1)	39.613(4)	25.207(3)	19.953(3)	15.545(2)
<i>c</i> , Å	14.062(3)	28.296(3)	17.004(2)	26.306(3)	25.966(4)	27.808(3)
α , °	90	90	90	90	90	87.14(1)
β , °	113.99(3)	90	98.36(1)	90	90	88.04(1)
γ , °	90	90	90	90	90	82.34(1)
<i>V</i> , Å ³	3418.4(12)	3440.2(6)	7419(1)	7851(2)	7022(2)	5456.8(9)
<i>Z</i>	8	8	16	16	16	12
ρ (calc.), g/cm ³	1.152	1.214	1.169	1.149	1.178	1.167
μ (Mo- <i>K</i> α), mm ⁻¹	0.06	0.07	0.06	0.06	0.06	0.06
Reflections collected	22483	40941	79498	26 973	80043	77 737
Independent reflections	7885, 5849 ^b	5104, 4595 ^b	17045, 10284 ^b	5614, 4872 ^b	9324, 7095 ^a	28869, 22311 ^b
<i>R</i> _{int}	0.040	0.041	0.061	0.058	0.056	0.035
Parameters	433	466	945	576	467	1400
<i>R</i> (<i>F</i>) ^b	0.053	0.038	0.053	0.068	0.054	0.061
<i>wR</i> (<i>F</i> ²)	0.139	0.097	0.140	0.147	0.146	0.154

^a Chosen for consistency with ref. 11; the reduced cell corresponds to the P2₁/n setting with *c*=13.810(3) Å and β =111.52(3)°; ^b Reflections with *I*>2 σ (*I*)

References

1. For examples see: R.A. Wiesboeck and M.F. Hawthorne, *J. Am. Chem. Soc.*, 1964, **86**, 1642; M. F. Hawthorne, D. C. Young, P. M. Garrett, D. A. Owen, S. G. Schwerin, F. N. Tebbe and P. A. Wegner, *J. Am. Chem. Soc.* 1968, **90**, 862; H. Tomita, H. Luu and T. Onak, *Inorg. Chem.*, 1991, **30**, 812; M. A. Fox, A.E. Goeta, A.K. Hughes and A.L. Johnson, *J. Chem. Soc. Dalton Trans.*, **2002**, 2132; M.G. Davidson, M.A. Fox, T.G. Hibbert, J.A.K. Howard, A. Mackinnon, I.S. Neretin and K. Wade, *Chem. Commun.*, **1999**, 1649.
2. For examples see: M. F. Hawthorne, D. C. Young, T. D. Andrews, D. V. Howe, R. L. Pilling, A. D. Pitts, M. Reintjes, L.F. Warren and P.A. Wegner, *J. Am. Chem. Soc.*, 1968, **90**, 879; L.F. Warren and M.F. Hawthorne, *J. Am. Chem. Soc.*, 1968, **90**, 4823; J.L. Spencer, F.G.A. Stone and M. Green, *J. Chem. Soc., Chem. Commun.*, **1972**, 1178; D.M.P. Mingos, M.I. Forsyth and A.J. Welch, *J. Chem. Soc., Dalton Trans.*, **1978**, 1363; M. A. Fox, A.K. Hughes, A.L. Johnson and M.A.J. Paterson, *J. Chem. Soc. Dalton Trans.*, **2002**, 2132; H.M. Colquhoun, T.J. Greenhough and M.G.H. Wallbridge, *J. Chem. Soc. Dalton Trans.*, **1978**, 303; X.L.R. Fontaine, N.N. Greenwood, J.D. Kennedy, K. Nestor, M. Thornton-Pett, S. Heřmanek, T. Jelínek and B. Štíbr, *J. Chem. Soc., Dalton Trans.*, **1990**, 681; U. Gradler, A.S. Weller, A.J. Welch and D. Reed, *J. Chem. Soc., Dalton Trans.*, **1996**, 335.
3. For examples see: D.A. Brown, W. Clegg, H.M. Colquhoun, J.A. Daniels, I.R. Stephenson and K. Wade, *J. Chem. Soc., Chem. Commun.*, **1987**, 889. T.D. Getman, C.B. Knobler and M.F. Hawthorne, *J. Am. Chem. Soc.*, 1990, **112**, 4593. R. Coult, M. A. Fox, W. R. Gill, K. Wade and W. Clegg, *Polyhedron* 1992, 11, 2717. J. Llop, C. Viñas, J. M. Oliva, F. Teixidor, M. A. Flores, R. Kivekäs and R. Sillanpää, *J. Organomet. Chem.* **2002**, 657, 232. A. Laromaine, C. Viñas, R. Sillanpää and R. Kivekäs, *Acta Cryst. Sect. C* **2004**, C60, o524. J.M. Oliva, N.L. Allan, P.v.R. Schleyer, C.Viñas and F. Teixidor, *J. Am. Chem. Soc.*, 2005, **127**, 13538. A. S. Batsanov, M. A. Fox, T. G. Hibbert, J. A. K. Howard, R. Kivekäs, A. Laromaine, R. Sillanpää, C. Viñas and K. Wade, *Dalton Trans.*, **2004**, 3822; K. Chui, H-W. Li and Z. Xie, *Organometallics*, 2000, **19**, 5447.

-
4. L.A. Boyd, W. Clegg, R.C.B. Copley, M.G. Davidson, M.A. Fox, T.G. Hibbert, J.A.K. Howard, A. Mackinnon, R.J. Peace and K. Wade, *Dalton Trans.*, 2004, 2786.
 5. G.B. Dunks, R.J. Wiersema and M.F. Hawthorne, *J. Am. Chem. Soc.*, 1973, **95**, 3174. V.I. Stanko, T.A. Babushkina, V.A. Brattsev, T.P. Klimova, A.M. Alymov, A.M. Vassilyev and S.P. Knyazev, *J. Organomet. Chem.*, 1974, **78**, 313.
 6. For examples see: G.B. Dunks, M.M. McKown and M.F. Hawthorne, *J. Am. Chem. Soc.*, 1971, **93**, 2541. D.F. Dustin, G.B. Dunks and M.F. Hawthorne, *J. Am. Chem. Soc.*, 1973, **95**, 1109. W.J. Evans, G.B. Dunks and M.F. Hawthorne, *J. Am. Chem. Soc.*, 1973, **95**, 4565. A. Burke, D. Ellis, D. Ferrer, D.L. Ormsby, G.M. Rosair and A.J. Welch, *Dalton Trans.*, **2005**, 1716. D. Ellis, M.E. Lopez, R. McIntosh, G.M. Rosair, A.J. Welch and R. Quenardelle, *Chem. Commun.*, **2005**, 1348.
 7. M. V. Yarosh, T. V. Baranova, V. L. Shirokii, A. A. Érdman and N. A. Maier, *Élektrokimiya (Engl. Transl.)*, **1993**, 29, 1125; M. V. Yarosh, T. V. Baranova, V. L. Shirokii, A. A. Érdman and N. A. Maier, *Russian J. Electrochem.*, **1994**, 30, 366.
 8. M. A. Fox, C. Nervi, A. Crivello and P. J. Low, *Chem. Commun.*, 2007, 2372.
 9. Z.G. Lewis and A.J. Welch, *Acta Cryst. C*, 1993, **49**, 705.
 10. For examples see, T.D. McGrath and A.J. Welch, *Acta Cryst. C* 1995, **51**, 654. R.L. Thomas and A.J. Welch, *Polyhedron*, 1999, **18**, 1961; U. Venkatasubramanian, D.J. Donohoe, D. Ellis, B.T. Giles, S.A. Macgregor, S. Robertson, G.M. Rosair, A.J. Welch, A.S. Batsanov, L.A. Boyd, R.C.B. Copley, M.A. Fox, J.A.K. Howard and K. Wade, *Polyhedron*, 2004, **23**, 629. A.S. Batsanov, W. Clegg, R.C.B. Copley, M.A. Fox, W.R. Gill, R.S. Grimditch, T.G. Hibbert, J.A.K. Howard, J.A.H. MacBride and K. Wade, *Polyhedron*, 2006, **25**, 300. K. Vyakaranam, S. Li, C. Zheng and N.S. Hosmane, *Inorg. Chem. Commun.*, 2001, **4**, 180. C. Songkram, K. Takaishi, K. Yamaguchi, H. Kagechika and Y. Endo, *Tetrahedron Lett.*, 2001, **42**, 6365. V. Balema, S. Blaurock and E. Hey-Hawkins, *Z. Naturforsch B. Chem. Sci.*, 1998, **53**, 1273.

-
11. M.M. Fein, J. Bobinski, N. Myers, N. Schwartz and M.S. Cohen, *Inorg. Chem.*, 1963, **2**, 1111.
 12. Many known decaborane-arylalkyne reactions are listed in M.A. Fox, Polyhedral Carboranes. In: R. H. Crabtree and D. M. P. Mingos, Editors, *Comprehensive Organometallic Chemistry III*, Elsevier, Oxford (2007), Vol 3 (C.E. Housecroft, Volume Editor), p.49.
 13. P.W. Causey, T.R. Besanger and J.F. Valliant, *J. Med. Chem.*, 2008, **51**, 2833.
 14. J.W. Steed, *CrystEngComm*, **2003**, *5*, 169-179.
 15. C. P. Brock and L.L. Duncan, *Chem. Mater.*, **1994**, *6*, 1307.
 16. A. Gavezzotti and G. Fillippini, *J. Phys. Chem.*, **1994**, *98*, 4831.
 17. E.S. Alekseyeva, M. A. Fox, J.A.K. Howard, J.A.H. MacBride and K. Wade, *Appl. Organomet. Chem.*, 2003, **17**, 499.
 18. I.V. Glukhov, M.Y. Antipin and K.A. Lyssenko, *Eur. J. Inorg. Chem.*, 2004, 1379. M. Tsuji, *J. Org. Chem.*, 2004, **69**, 4063. W. Clegg, R. Coult, M. A. Fox, W. R. Gill, J. A. H. MacBride and K. Wade, *Polyhedron* **1993**, *12*, 2711. R. Kivekas, R. Sillanpaa, F. Teixidor, C. Viñas and R. Nuñez, *Acta Cryst. Sect. C* **1994**, *C50*, 2027.
 19. For PhNMe₂, M.J. Homer, K.T. Holman and M.D. Ward, *Angew. Chem. Int. Ed. Engl.*, 2001, **40**, 4045. PhNH₂, M. Fukuyo, K. Hirotsu and T. Higuchi, *Acta Cryst. B*, 1982, **38**, 640.
 20. M.A. Fox, J. A. H. MacBride, R.J. Peace and K. Wade, *J. Chem. Soc. Dalton Trans.*, 1998, 401.
 21. S. Heřmanek, *Inorg. Chim. Acta*, 1999, **289**, 20.
 22. C. Hansch, A. Leo and R.W. Taft, *Chem. Rev.* 1991, **91**, 165.
 23. L.A. Leites, L.E. Vinogradova, V.N. Kalinin and L.I. Zakharkin, *Bull. Acad. Sci. USSR, Div. Chem. Sci.*, 1970, 2437.
 24. T. Inagaki, *J. Chem. Phys.*, 1972, **57**, 2526.
 25. Carborane radicals with a 2n+3 skeletal electron count are extremely rare with only one structurally characterised so far. X. Fu, H.-S. Chan and Z. Xie, *J. Am. Chem. Soc.*, 2007, **129**, 8964.
 26. D.A. Brown, H.M. Colquhoun, J.A. Daniels, J. A. H. MacBride, I.R. Stephenson and K. Wade, *J. Mater. Chem.*, 1992, **2**, 793.

-
27. Y. Endo, C. Songkram, R. Yamasaki, A. Tanatani, H. Kagechika, K. Takaishi and K. Yamaguchi, *J. Organomet. Chem.*, 2002, **657**, 48.
28. O.O. Sogbein, A.E.C. Green, P. Schaffer, R. Chankalal, E. Lee, B.D. Healy, P. Morel and J.F. Valliant, *Inorg. Chem.*, 2005, **44**, 9574.
29. *SHELXTL*, Version 5.10. Bruker AXS: Madison, Wisconsin, USA, 1997.
30. Gaussian 03, Revision C.02, M. J. Frisch, G. W. Trucks, H. B. Schlegel, G. E. Scuseria, M. A. Robb, J. R. Cheeseman, J. A. Montgomery, Jr., T. Vreven, K. N. Kudin, J. C. Burant, J. M. Millam, S. S. Iyengar, J. Tomasi, V. Barone, B. Mennucci, M. Cossi, G. Scalmani, N. Rega, G. A. Petersson, H. Nakatsuji, M. Hada, M. Ehara, K. Toyota, R. Fukuda, J. Hasegawa, M. Ishida, T. Nakajima, Y. Honda, O. Kitao, H. Nakai, M. Klene, X. Li, J. E. Knox, H. P. Hratchian, J. B. Cross, C. Adamo, J. Jaramillo, R. Gomperts, R. E. Stratmann, O. Yazyev, A. J. Austin, R. Cammi, C. Pomelli, J. W. Ochterski, P. Y. Ayala, K. Morokuma, G. A. Voth, P. Salvador, J. J. Dannenberg, V. G. Zakrzewski, S. Dapprich, A. D. Daniels, M. C. Strain, O. Farkas, D. K. Malick, A. D. Rabuck, K. Raghavachari, J. B. Foresman, J. V. Ortiz, Q. Cui, A. G. Baboul, S. Clifford, J. Cioslowski, B. B. Stefanov, G. Liu, A. Liashenko, P. Piskorz, I. Komaromi, R. L. Martin, D. J. Fox, T. Keith, M. A. Al-Laham, C. Y. Peng, A. Nanayakkara, M. Challacombe, P. M. W. Gill, B. Johnson, W. Chen, M. W. Wong, C. Gonzalez, and J. A. Pople, Gaussian, Inc., Wallingford CT, 2004.
31. T. P. Onak, H. L. Landesman and R. E. Williams, *J. Phys. Chem.*, 1959, **63**, 1533.